# Linearized Discrete-Time Model of Higher Order Charge-Pump PLLs

Chuang Bi, Paul F. Curran, and Orla Feely
School of Electrical, Electronic and Mechanical Engineering, University College Dublin, Belfield, Dublin 4, Ireland
Email: chuang.bi@ucd.ie, paul.curran@ucd.ie, orla.feely@ucd.ie

***Abstract*—In this paper, we derive linearized discrete-time models of higher order Charge-Pump Phase-Locked Loops (CP-PLLs). The behaviour of CP-PLLs in the steady state is analysed and an important feature is developed. The nonlinear state equations of CP-PLLs are linearized around the equilibrium point. The linearized discrete-time model is finally verified using behavioral simulations in Matlab and PSpice.**

## I. Introduction

Charge-Pump Phase Locked Loops (CP-PLLs) are important component blocks which are used in a wide variety of applications, such as clock generation, frequency synthesis and clock data recovery. The popularity of CP-PLLs is due to the fact that they provide flexible design parameters, such as loop bandwidth, damping factor and locking range. In Gardner's pioneering work on CP-PLLs [1], he develops what has become the standard linear model and provides some empirical design rules. Subsequently many analytic models for CP-PLLs have been proposed. Van Paemel [2], Acco [3], Hedayat [4] and Co [5] have given nonlinear models for second order loops. Hedayat [6], Hanumolu [7], Wang [8] and Daniels [9] have analysed third order CP-PLLs while Guermandi [10] and Yao [11] have studied fourth order CP-PLLs. In the present work we consider quite general $n$th order CP-PLLs.

The work of Van Paemel [2] in particular is of interest here. Van Paemel establishes that for first order loop filter the system permits a model which is of second order and discrete-time, although not in fact linear. Van Paemel shows that, close to equilibrium, the system behaves according to one of four particular modes determined by the patterns of transitions of the VCO and the PFD. We establish that in the more general case of higher order filters the system is again described by a discrete-time system of order equal to one plus the order of the filter and that the behaviour close to equilibrium is again described by four modes, indeed the same four modes discussed by Van Paemel. As stated, the system described by Van Paemel is not in fact linear or even linearizable. It transpires that, given a first order filter, the designer must choose between having a capacity to lock or being linearizable, they cannot have both. In the case of higher order filters however the designers can, and essentially do, choose to design systems which can lock and which are linearizable. Since engineers are particularly interested in the local dynamics around the equilibrium point, they generally develop linearized discrete-time models of CP-PLLs and it is therefore of some comfort to know that such models exist and are valid.

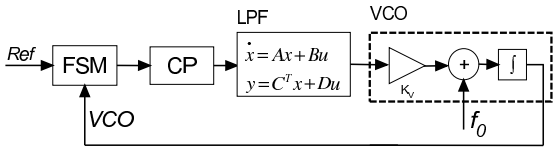


Fig. 1. A block diagram of charge-pump phase-locked loops.

This paper is organized in the following manner. Section II briefly describes the behavior of CP-PLLs in the steady state. The complete analysis of the linearized discrete-time model of CP-PLLs around the equilibrium point is presented in section III. Section IV presents some simulation results from Matlab and PSpice.

## II. Analysis of CP-PLLs in the steady state

Charge-Pump Phase-locked Loops (CP-PLLs) are composed of a phase and frequency detector (PFD), a charge pump (CP), a loop filter (LPF) and a voltage-controlled oscillator (VCO). The PFD is treated as a finite state machine (FSM) which compares the phase and frequency of the VCO signal and the external reference signal. The state transitions are triggered by the rising edge of the VCO signal ($VCO\uparrow$) and the reference signal ($Ref\uparrow$). The states of the FSM are denoted by $(1,0)$, $(0,0)$ and $(0,1)$. The PFD outputs Up and Down signals which are proportional to the phase error. The CP circuit is controlled by the Up and Down signal and generates output $I_p$, $0$ or $-I_p$, where $I_p$ is the charge pump current. The LPF is described by the state-space equation

$$\dot{x} = Ax + Bu \tag{1}$$

$$y = C^T x + Du \tag{2}$$

where $x$ is an $n\times 1$ vector ($n \geq 1$), $u$ is an input scalar, which is $I_p$, $0$ or $-I_p$, and $y$ is an output scalar. $A$, $B$, $C^T$ and $D$ are, respectively, $n\times n$, $n\times 1$, $1\times n$, and $1\times 1$ constant matrices.

The input of the VCO is the output of the LPF, $y$, and changes the frequency of the VCO. So the frequency of the VCO is given by $f_{VCO}(t) = f_0 + K_v y(t)$ , where $K_v$ is the VCO gain, expressed in $Hz/V$ and $f_0$ is the initial frequency of the VCO. The associated phase of the VCO is $\theta_{VCO}(t) = \int_0^t f_{VCO}(\tau)d\tau$.

Van Paemel [2] categorized the dynamic behavior of CP-PLLs into six cases, depending on the relationship between the phase and frequency of the VCO and reference signals. We assume that the CP-PLL is close to locking state. We consider four cases for the local dynamics around the equilibrium point,

as shown in Fig. 2. We define that the rising edges of the reference signal occur at the times $t = kT$ for all integers $k$, where $T = 1/f_{ref}$ is the period of the reference signal. Similarly, we denote that the times at which the falling edges of VCO occur by $t = t_k$, and introduce the variable $\tau_k = t_k - kT$. Another variable is the voltage across the capacitors sampled at the later of the two times $t = kT$ and $t = t_k$, i.e. $x_k = x(max\{kT, t_k\})$. Firstly, we consider the case when the CP-PLL is in the steady state and the system is at the equilibrium point. The FSM is in the state $(0, 0)$ for all the time $t$ and $t_k = kT$ for all $k$. The LPF input, $u$, equals 0. The state equations (1) and (2) become

$$\dot{x} = Ax \tag{3}$$

$$y = C^T x \tag{4}$$

We obtain the solution of (3) and (4) for $kT \le t \le (k+1)T$ as follows:

$$x(t) = e^{A(t-kT)}x(kT) \tag{5}$$

$$\begin{aligned}\theta_{VCO}(t) &= \int_{kT}^{t}(f_0 + K_v C^T e^{A(\tau-kT)}x(kT))d\tau \\ &= f_0(t-kT) + K_v C^T(\int_0^{t-kT} e^{A\tau}d\tau)x(kT)\end{aligned} \tag{6}$$

At the equilibrium point, we define $x(kT) = x^*$ for all $k$ and put $t = (k+1)T$ into the equations (5) and (6). We obtain an important feature of the system at the equilibrium point from the equation (6):

$$T(f_0 + K_v C^T x^*) = 1 \tag{7}$$

From the equation (5), we obtain $x^* = e^{AT}x^*$ and conclude that $e^{AT}$ has an eigenvalue at 1 with the associated eigenvector, $x^*$ and $A$ has an eigenvalue at 0 with the associated eigenvector, $x^*$.

## III. Linearized discrete-time models of CP-PLLs

In this section we derive the linearized discrete-time model for the higher order CP-PLLs based on the Van Paemel's paper [2]. In order to conveniently obtain linearized discrete-time models of CP-PLLs, we firstly introduce the following normalized variables:

$$\hat{\tau}_k = \tau_k/T \text{ and } \hat{x}_k = x_k - x^*. \tag{8}$$

### A. $\hat{\tau}_k > 0$, $\hat{\tau}_{k+1} > 0$

We define $x_k = x(t_k)$ and $x_{k+1} = x(t_{k+1})$ in the case $A$, as shown in Fig. 2 (a). The rising edge of the VCO lags behind the rising edge of the reference signal and the state of the FSM is $(1, 0)$ when the time is from $kT$ to $t_k$. The input of LPF, $u$, equals $I_p$. The equation (1) becomes $\dot{x} = Ax + BI_p$ and the solution is

$$x(t_k) = x(kT) + (Ax(kT) + BI_p)T\hat{\tau}_k \tag{9}$$

When time is from $t_k$ to $(k+1)T$, the state of the FSM is $(0, 0)$ and $u$ equals to 0. The equation (1) becomes $\dot{x} = Ax$ and the solution is

$$x((k+1)T) = e^{AT(1-\hat{\tau}_k)}x_k \tag{10}$$

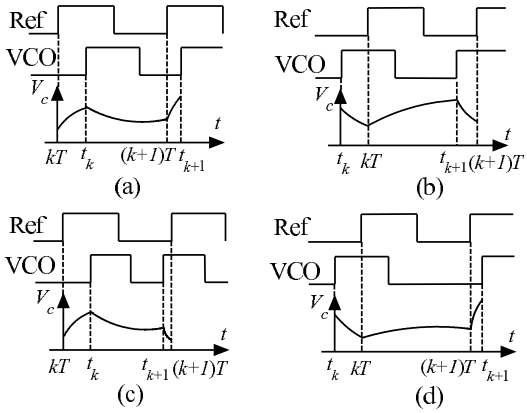


Fig. 2. Waveforms for the four cases.

When time is from $(k+1)T$ to $t_{k+1}$, the state of the FSM is $(1, 0)$ and $u$ equals to $I_p$ and the solution of the equation (1) is

$$\begin{aligned}x(t_{k+1}) &= x((k+1)T) + \\ &(Ax((k+1)T) + BI_p)T\hat{\tau}_{k+1}\end{aligned} \tag{11}$$

We put the equation (10) into the equation (11) and obtain

$$x(t_{k+1}) = e^{AT(1-\hat{\tau}_k)}x_k + (Ae^{AT(1-\hat{\tau}_k)}x_k + BI_p)T\hat{\tau}_{k+1} \tag{12}$$

Using the equation (8) and neglecting the higher order terms at the equilibrium point, we obtain the difference equation for $\hat{x}_{k+1}$ from the equation (12)

$$\hat{x}_{k+1} = e^{AT}\hat{x}_k + BI_pT\hat{\tau}_{k+1} \tag{13}$$

Now we define another function $\Phi_{VCO}(t)$ which is a function of $\theta_{VCO}(t)$ mod $2\pi$. The $k^{th}$ rising edge of the VCO occur at the time $t_k$ when $\Phi_{VCO}(t_k)$ equals 1.

As shown in Fig. 2 (a), the rising edge of the VCO occurs at the time $t_{k+1}$, so we can get

$$\begin{aligned}\Phi_{VCO}(t_{k+1}) &= \int_{(k+1)T}^{t_{k+1}}(f_0 + K_v C^T x((k+1)T) + K_v DI_p)dt \\ &+\Phi_{VCO}((k+1)T) = 1\end{aligned} \tag{14}$$

$\hat{\tau}_{k+1}$ is computed as

$$\hat{\tau}_{k+1} = \frac{1 - \Phi_{VCO}((k+1)T)}{f_0T + K_v DI_pT + K_v TC^T x((k+1)T)} \tag{15}$$

On the other hand, $\Phi_{VCO}((k+1)T)$ is given by

$$\begin{aligned}\Phi_{VCO}((k+1)T) &= \int_{t_k}^{(k+1)T}(f_0 + K_v C^T e^{A(t-t_k)}x_k)dt \\ &= 1 - \hat{\tau}_k + q^T\hat{x}_k\end{aligned} \tag{16}$$

where $q^T = K_v C^T \int_0^T e^{A\tau}d\tau$.

We put the equations (16) and (8) into the equation (15) and get

$$\hat{\tau}_{k+1} = \frac{\hat{\tau}_k - q^T\hat{x}_k}{f_0T + K_v DI_pT + K_v TC^T e^{AT(1-\hat{\tau}_k)}(\hat{x}_k + x^*)} \tag{17}$$

Using the equation (7) and neglecting the higher order terms at the equilibrium point, we obtain $\hat{\tau}_{k+1}$ from the equation (17).

$$\hat{\tau}_{k+1} = \frac{\hat{\tau}_k - q^T \hat{x}_k}{1 + K_v D I_p T} \tag{18}$$

for $\hat{\tau}_k > 0$, $\hat{\tau}_k > q^T \hat{x}_k$.

*B.* $\hat{\tau}_k < 0$, $\hat{\tau}_{k+1} < 0$

In this case (Fig. 2 (b)), we define $x_k = x(kT)$ and $x_{k+1} = x((k+1)T)$. The input of LPF, $u$, equals 0 from $kT$ to $t_{k+1}$ and $-I_p$ from $t_{k+1}$ to $(k+1)T$. According to the state equations (1), $x(t_{k+1})$ and $x((k+1)T)$ are expressed as follows:

$$x(t_{k+1}) = e^{A(t_{k+1}-kT)} x_k \tag{19}$$

$$x((k+1)T) = x(t_{k+1}) + (Ax(t_{k+1}) - BI_p)((k+1)T - t_{k+1}) \tag{20}$$

Using the equations (7), (8), (19) and (20) and neglecting the higher order terms at the equilibrium point, we can get the same result for $\hat{x}_{k+1}$ as in case $A$:

$$\hat{x}_{k+1} = e^{AT} \hat{x}_k + BI_p T \hat{\tau}_{k+1} \tag{21}$$

We know the rising edge of the VCO occurs at the time $t_{k+1}$ from Fig. 2 (b). We obtain

$$\begin{aligned} \Phi_{VCO}(t_{k+1}) = & \int_{t_k}^{kT} (f_0 + K_v C^T x(t) - K_v D I_p) dt \\ & + \int_{kT}^{t_{k+1}} (f_0 + K_v C^T x(t)) dt = 1 \end{aligned} \tag{22}$$

We put the equations (7), (8), (19) and (20) into the equation (22) and compute $\hat{\tau}_{k+1}$ in this case as

$$\hat{\tau}_{k+1} = (1 - K_v D I_p T)\hat{\tau}_k - q^T \hat{x}_k \tag{23}$$

for $\hat{\tau}_k < 0$, $(1 - K_v D I_p T)\hat{\tau}_k < q^T \hat{x}_k$.

*C.* $\hat{\tau}_k > 0$, $\hat{\tau}_{k+1} < 0$

We define $x_k = x(t_k)$ and $x_{k+1} = x((k+1)T)$ in the case $C$ shown in Fig. 2 (c). The input of LPF, $u$, equals 0 from $t_k$ to $t_{k+1}$ and $-I_p$ from $t_{k+1}$ to $(k+1)T$. The solution of the state equation (1) are expressed at times $t_{k+1}$ and $(k+1)T$ as follows:

$$x(t_{k+1}) = e^{A(t_{k+1}-t_k)} x_k \tag{24}$$

$$x((k+1)T) = x(t_{k+1}) + (Ax(t_{k+1}) - BI_p)((k+1)T - t_{k+1}) \tag{25}$$

Using the equations (7), (8), (24) and (25), we can get the same result for $\hat{x}_{k+1}$ as in case $A$:

$$\hat{x}_{k+1} = e^{AT} \hat{x}_k + BI_p T \hat{\tau}_{k+1} \tag{26}$$

In this case, we know that the rising edge of the VCO occurs at the time $t_{k+1}$ , as shown in Fig. 2 (c). We obtain

$$\Phi_{VCO}(t_{k+1}) = \int_{t_k}^{t_{k+1}} (f_0 + K_v C^T e^{A(t-t_k)} x_k) dt = 1 \tag{27}$$

Using the equation (7) and neglecting the higher order terms at the equilibrium point, $\hat{\tau}_{k+1}$ is computed in this case as

$$\hat{\tau}_{k+1} = \hat{\tau}_k - q^T \hat{x}_k \tag{28}$$

for $\hat{\tau}_k > 0$, $\hat{\tau}_k < q^T \hat{x}_k$.

*D.* $\hat{\tau}_k < 0$, $\hat{\tau}_{k+1} > 0$

We define $x_k = x(kT)$ and $x_{k+1} = x(t_{k+1})$ in the case $D$ shown in Fig. 2 (d). The input of LPF, $u$, equals 0 from $kT$ to $(k+1)T$ and $I_p$ from $(k+1)T$ to $t_{k+1}$. The solution of the state equation (1) are expressed at times $(k+1)T$ and $t_{k+1}$ as follows:

$$x((k+1)T) = e^{AT} x_k \tag{29}$$

$$\begin{aligned} x(t_{k+1}) = & x((k+1)T) + \\ & (Ax((k+1)T) + BI_p)(t_{k+1} - (k+1)T) \end{aligned} \tag{30}$$

Using the equations (7), (8), (29) and (30) and neglecting the higher order terms at the equilibrium point, we can get the same result for $\hat{x}_{k+1}$ as in case $A$:

$$\hat{x}_{k+1} = e^{AT} \hat{x}_k + BI_p T \hat{\tau}_{k+1} \tag{31}$$

Fig. 2 (d) shows that the rising edge of VCO occurs at the time $t_{k+1}$. We obtain

$$\begin{aligned} \Phi_{VCO}(t_{k+1}) = & \int_{t_k}^{kT} (f_0 + K_v C^T x(t) - K_v D I_p) dt \\ & + \int_{kT}^{(k+1)T} (f_0 + K_v C^T x(t)) dt \\ & + \int_{(k+1)T}^{t_{k+1}} (f_0 + K_v C^T x(t) + K_v D I_p) dt \\ & = 1 \end{aligned} \tag{32}$$

We put the equations (7), (8), (29) and (30) into the equation (32) and compute $\hat{\tau}_{k+1}$ in this case as

$$\hat{\tau}_{k+1} = \frac{(1 - K_v D I_p)\hat{\tau}_k - q^T \hat{x}_k}{1 + K_v D I_p T} \tag{33}$$

for $\hat{\tau}_k < 0$, $(1 - K_v D I_p T)\hat{\tau}_k > q^T \hat{x}_k$. Finally, linearized discrete-time models of higher order CP-PLLs are presented by the equations (34) and (35):

$$\hat{x}_{k+1} = e^{AT} \hat{x}_k + BI_p T \hat{\tau}_{k+1} \tag{34}$$

$$\hat{\tau}_{k+1} = \begin{cases} \frac{\hat{\tau}_k - q^T \hat{x}_k}{1 + K_v D I_p T} & \text{for } \hat{\tau}_k > 0,\ \hat{\tau}_k > q^T \hat{x}_k \\ (1 - K_v D I_p T)\hat{\tau}_k - q^T \hat{x}_k & \\ \qquad\qquad & \text{for } \hat{\tau}_k < 0,\ \hat{\tau}_k < \frac{q^T \hat{x}_k}{1 - K_v D I_p T} \\ \hat{\tau}_k - q^T \hat{x}_k & \text{for } \hat{\tau}_k > 0,\ \hat{\tau}_k < q^T \hat{x}_k \\ \frac{(1 - K_v D I_p)\hat{\tau}_k - q^T \hat{x}_k}{1 + K_v D I_p T} & \\ \qquad\qquad & \text{for } \hat{\tau}_k < 0,\ \hat{\tau}_k > \frac{q^T \hat{x}_k}{1 - K_v D I_p T} \end{cases} \tag{35}$$

## IV. Behavioral simulation

The linearized discrete-time model in the previous section is now verified in Pspice. Though the linearized model is suitable for higher order CP-PLLs, we choose the third order CP-PLL as an example in this section because of the popularity of the third order CP-PLL frequency synthesizer in the practical design.

Consider the second-order LPF, we can get

$$A = \begin{bmatrix} -\tau_2 & \tau_2 \\ \tau_1 & -\tau_1 \end{bmatrix},\ B = \begin{bmatrix} \frac{1}{C_3} \\ 0 \end{bmatrix},\ C^T = [1,\ 0],\ D = [0]$$

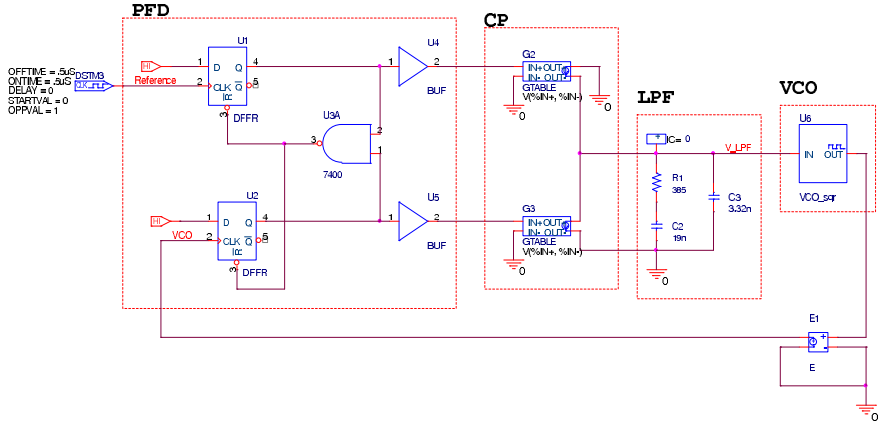


Fig. 3. Simulation circuit for charge-pump phase-locked loops in Pspice.

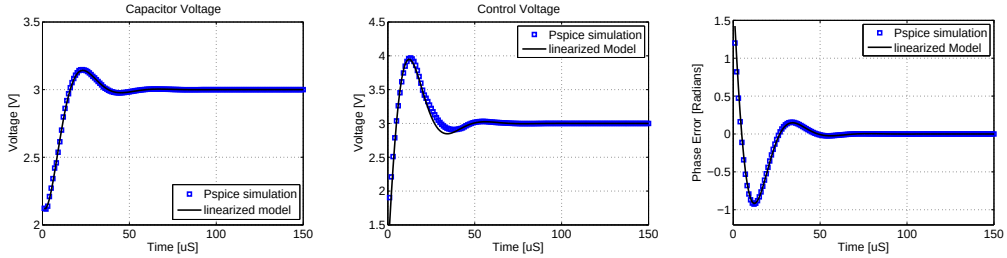


(a) (b) (c)

Fig. 4. Simulation results obtained from linearized discrete-time model and PSpice simulation. (a) the capacitor voltage; (b) the control voltage; (c) the phase error.

where $\tau_1 = \frac{1}{R_1 C_2}$, $\tau_2 = \frac{1}{R_1 C_3}$ and $R_1$, $C_2$, $C_3$ are the circuit parameters of LPF, as shown in Fig. 3. Then we put these constant matrices into the equations (34) and (35) to get the linearized discrete-time model of the third order CP-PLL. For this particular case when $D = [0]$, the equation (35) becomes $\hat{\tau}_{k+1} = \hat{\tau}_k - q^T \hat{x}_k$.

We build up a third order CP-PLL in the Pspice environment, which is shown in Fig. 3. The circuit parameters, like those in the linearized discrete-time model, are given $I_p = 5mA$, $K_v = 0.1MHz/V$, $f_{ref} = 1MHz$, $R_1 = 385\Omega$, $C_2 = 19.2nF$, $C_3 = 3.32nF$. In order to verify the linearized discrete-time model of CP-PLLs, we choose the initial values around the equilibrium point, the capacitor voltage $V_{C_2}(0) = 3.005V$, the control voltage $V_{C_3}(0) = 3.005V$ and the phase error $\Phi_e(0) = 0$. The linearized discrete-time model of the third order CP-PLL, the equations (34) and (35), described in section III is simulated using Matlab. The validity of the linearized discrete-time model around the equilibrium point is verified by comparing the capacitor and control voltage and the phase error obtained from Matlab and Pspice simulation, as shown in Fig. 4.

## V. Conclusions

The linearized discrete-time model of higher order CP-PLLs around equilibrium has been described in this paper, based on Van Paemel's paper [2]. We have linearized the nonlinear model around equilibrium and developed explicitly a more general linearized discrete-time model for the CP-PLLs. We, then, have presented the simulation results obtained from Matlab and PSpice simulation to verify the validity of this linearized model. We have investigated the local dynamics around equilibrium when the CP-PLL is close to the locking state, which engineers are particularly interested in.

## References


[1] F. Gardner, "Charge-pump phase-lock loops," *IEEE Trans. Commun.*, vol. 28, no. 11, pp. 1849–1858, Nov. 1980.

[2] M. Van Paemel, "Analysis of a charge-pump PLL: A new model," *IEEE Trans. Commun.*, vol. 42, no. 7, pp. 2490–2498, Nov. 1994.

[3] P. Acco, "Why do we linearise charge pump pll equation so early?" in *Proc. NDES*, May 2001, pp. 173–176.

[4] C. D. Hedayat, A. Hachem, Y. Leduc, and G. Benbassat, "High-level modeling applied to the second-order charge-pump PLL circuit," *Texas Instruments Technical Journal*, vol. 14, no. 2, Mar. 1997.

[5] R. S. Co and J. H. Mulligan, "Optimization of phase-locked loop performance in data recovery systems," *IEEE J. Solid-State Circuits*, vol. 29, pp. 1022–1034, Sep. 1994.

[6] C. D. Hedayat, A. Hachem, Y. Leduc, and G. Benbassat, "Modeling and characterization of the 3rd order charge-pump PLL: a fully event-driven approach," *Analog Integrated Circuits and Signal Processing*, vol. 19, no. 1, pp. 25–45, Apr. 1999.

[7] P. K. Hanumolu, M. Brownlee, K. Mayaram, and U.-K. Moon, "Analysis of charge-pump phase-locked loops," *IEEE Trans. Circuits Syst. I*, vol. 51, no. 9, pp. 1665–1674, Sep. 2004.

[8] Z. D. Wang, "An analysis of charge-pump phase-locked loops," *IEEE Trans. Circuits Syst. I*, vol. 52, no. 10, pp. 2128–2138, Oct. 2005.

[9] B. Daniels and R. Farrell, "Rigorous stability criterion for digital phase locked loops," *ISAST Trans. on Electronics and Signal Processing*, vol. 2, pp. 1–10, 2008.

[10] M. Guermandi, E. Franchi, and A. Gnudi, "On the simulation of fast settling charge pump plls up to fourth order," *International Journal of Circuit Theory and Applications*, Apr. 2010.

[11] C.-Y. Yao, C.-T. Hsu, and C.-C. Hsieh, "Stability analysis of fourth-order charge-pump plls using linearized discrete-time models," *in Proc. 2007 IEEE Region 10 Conference*, pp. 1–4, 2007.